J Mater Sci (2010) 45:2419–2426
DOI 10.1007/s10853-010-4209-x

Crystal structure refinement of A-type carbonate apatite by X-ray powder diffraction

Toru Tonegawa · Toshiyuki Ikoma · Tomohiko Yoshioka · Nobutaka Hanagata · Junzo Tanaka

Received: 14 November 2009 / Accepted: 5 January 2010 / Published online: 14 January 2010

Abstract Complete carbonate substitution at A-sites (OH) of low-crystallinity hydroxyapatite with near stoichiometric composition (i.e. Ca/P ratio of 1.65) was achieved by heating in a dry carbon dioxide flow at 1173 K for 64 h. The carbonate content was analysed by thermogravimetry and infrared absorption spectrometry; the chemical composition was determined to be $Ca_{9.9\pm0.1}(PO_4)_{6.00\pm0.1}(CO_3)_{0.9\pm0.1}$. The crystal structure and atomic configuration of the carbonate ion were determined by Rietveld refinement using X-ray powder diffraction data. This analysis revealed that the space group was monoclinic *Pb* with $a = 0.9571(1)$, $b = 1.9085(2)$, $c = 0.68755(3)$ nm and $\gamma = 119.847(7)°$. The triangular planes of the carbonate ions were oriented parallel to the *c*- and *a*-axes, though there were two independent carbonate sites with occupancy factors of 0.56(1) and 0.34(1), where the triangles were oppositely rotated about the corresponding carbon atoms by 23° and −18°, respectively. The arrangement of the ions was disordered, which explains the lack of a thermal phase transition below 623 K.

Electronic supplementary material The online version of this article (doi:10.1007/s10853-010-4209-x) contains supplementary material, which is available to authorized users.

T. Tonegawa · T. Yoshioka · J. Tanaka
Graduate School of Science & Engineering,
Tokyo Institute of Technology, O-okayama 2-12-1,
Meguro-ku, Tokyo 152-8550, Japan

T. Ikoma (✉) · N. Hanagata
Biomaterials Center, National Institute for Materials Science,
Sengen 1-2-1, Tsukuba, Ibaraki 305-0047, Japan
e-mail: IKOMA.Toshiyuki@nims.go.jp

Introduction

Hydroxyapatite ($Ca_{10}(PO_4)_6(OH)_2$, HAp) exists in partially carbonated form as the main inorganic component of bone and teeth [1, 2]. Three types of carbonate apatites (CAp) are known, classified on the basis of the substitution sites: A-type, where carbonate ions occupy OH sites; B-type, where they occupy PO_4 sites; and AB-type, where they occupy both OH and PO_4 sites. The chemical properties of CAp are of great importance in the design of novel biodegradable ceramics, cements and CAp/polymer composites [3], since the chemical bonds in the apatite lattice are weakened by increase in the amount of carbonate and the dissolution rate is particularly increased [4, 5]. Furthermore, CAp shows the better biocompatibility [6]. However, the crystal structure of CAp has not yet been studied in detail; the configuration and arrangement (ordered/disordered) of carbonate ions remains controversial in relation to the existence of thermal phase transition.

We previously described the crystal structures of A-type CAp powders with different amounts of carbonate. Rietveld refinement showed that A-type CAp with the chemical formula $Ca_{10.0}(PO_4)_{6.00}[O_{0.2}, (CO_3)_{0.8}]$ had the hexagonal space group $P\bar{6}$ with $a = 0.95324$ and $c = 0.68882$ nm [7]. The crystal structure was almost coincident with that determined for single crystals [8, 9]—the carbonate ions occupied three equivalent positions, resulting in threefold rotational disordered arrangement [7, 9]. From X-ray powder diffraction (XRD) analyses, Elliott et al. [10] concluded that completely carbonated A-type CAp had monoclinic symmetry with space group *Pb* with $a = 0.9557$, $b \approx 2a$, $c = 0.6872$ nm and $\gamma = 120.36°$. On the contrary, Fleet and Liu [11, 12] showed that A-type CAp with the chemical composition $Ca_{10}(PO_4)_6[(CO_3)_{0.75}(OH)_{0.5}]$ had the lattice parameters $a = 0.9522$ and $c = 0.6875$ nm.

A single crystal synthesised at 2 GPa and 1400–1500 °C from $Ca_2P_2O_7$, CaO and $CaCO_3$ had a new trigonal symmetry and belonged to space group $P\bar{3}$. These results suggest that the crystal structure of A-type CAp depends on the chemical composition. To our knowledge, the atomic coordination of monoclinic A-type CAp has not been determined.

A-type CAp with almost stoichiometric composition, i.e. $Ca_{10}(PO_4)_6[(OH)_{2-2x},(CO_3)_x]$ with $x > 0.9$, exhibits thermal phase transition from monoclinic to hexagonal symmetry near 473 K with the disappearance of *b*-glide planes [13–16]. However, the existence of this thermal phase transition has not been described in detail.

In the present study, A-type CAp powder was prepared by heating stoichiometric low-crystallinity HAp powder in a dry carbon dioxide flow. In the resultant powder, only the A-sites were completely substituted by carbonate ions. The crystal structure and the arrangement (ordered/disordered) of the carbonate ions were determined by Rietveld refinement using powder XRD data. The thermal phase transition was investigated by differential scanning calorimetry (DSC).

Experimental

HAp was synthesised by a wet method from a $Ca(OH)_2$ suspension and a H_3PO_4 solution. The details of the preparation method are described elsewhere [17]. The HAp precipitate obtained was filtered and dried at 333 K; it was then heated at 1173 K for 64 h in a carbon dioxide flow (500 mL/min). (The gas used here was sufficiently dried through active Al_2O_3 at both the inlet and outlet.) The concentrations of Ca^{2+} and PO_4^{3-} were determined by an inductive coupled plasma emission spectrometer (ICP, SII Inc., VISTA-MPX). The powder was dissolved in 0.001 mol/L of hydrochloric acid.

The carbonate content was analysed by thermogravimetry (TG, Rigaku Co. Ltd., Thermo plus 8120) between 298 and 1723 K at a heating rate of 10 K/min in air using a platinum sample holder. Alumina was used as the reference sample; the sample weight was about 10 mg.

The infrared (IR) absorption spectrum was measured at room temperature with a JASCO FT/IR-8000 spectrometer in the range 400–4000 cm^{-1} to identify the sites occupied by carbonate ions and the existence of OH ions. Transparent samples were prepared by a KBr pellet method with the ratio A-type CAp to KBr being 1:200.

DSC measurements (Perkin-Elmar, Pyris 1) were conducted to confirm the existence of thermal phase transition between 400 and 600 K with heating and cooling rates of 20 K/min using an aluminium sample holder; the sample weight was 32.7 mg.

XRD intensity data were collected at room temperature using a Rigaku RAD-rC diffractometer with graphite-monochromatised Cu Kα radiation at 50 kV and 150 mA. The measurements were repeated twice in the 2θ range 10°–110° in steps of 0.02° with a counting time of 4 s. The crystal structure was refined for the averaged intensity data using RIETAN-2000 [18]. Rietveld refinements were conducted for two different carbonate arrangements on the basis of space group *Pb*: ordered and disordered arrangements. Initial unit cell parameters and atomic coordinates were quoted from those refined for space group $P\bar{6}$ [7]. Four constraints were applied for iterative calculations to avoid unnecessary divergence: (1) C–O distances were always kept within the range 0.130 ± 0.02 nm, (2) O–C–O angles within 120° ± 2°, (3) P–O distances within 0.155 ± 0.02 nm and (4) O–P–O angles within 109.47° ± 2°. Occupancy factors *g* for atomic sites were fixed at 1.0 without those of atoms in the carbonate group. For the disordered carbonate arrangement, the values of *g* for two crystallographic independent sites, C(a) and C(b), were refined for the sum to be 0.9: The value of *g* for C(a) was equal to those for O(a1), O(a2) and O(3a); the value for C(b) was obtained by subtracting the value for C(a) from 0.9 and was equal to those of O(b1), O(b2) and O(b3). The individual thermal parameters of the O and C atoms in the carbonate group were fixed at 0.008 nm^2, and the other common thermal parameters were adopted for equivalent atoms, e.g. 0.012, 0.011 and 0.009 nm^2 for Ca, P and O, respectively. Finally, the atomic coordination, thermal parameters and *g* value for the C(a) atom were refined simultaneously.

Results and discussion

Chemical composition and site occupied by carbonate

The chemical composition is essential for determining *g* because individual thermal parameters are strongly correlated to *g*. ICP analyses revealed that the Ca and PO_4 contents were nearly stoichiometric: the accurate Ca/P ratio determined experimentally was 1.65. The carbonate content was analysed by TG measurement, as shown in Fig. 1. TG weight loss ascribed to the evolution of carbon dioxide began to increase at 873 K and continued up to 1723 K. The evolution of CO_2 from A-type CAp and H_2O from HAp completed at 1723 K [19], leaving behind an oxyapatite. The total loss was 4.0 ± 0.3 wt%, which is almost equal to the ideal value of 4.27 wt% for A-type CAp ($Ca_{10}(PO_4)_6(CO_3) \rightarrow Ca_{10}(PO_4)_6O + CO_2$).

IR absorption bands were observed as shown in Fig. 2. In general, the carbonate bands at 870–880 cm^{-1} correspond to the out-of-plane bending mode (υ_2), and those at

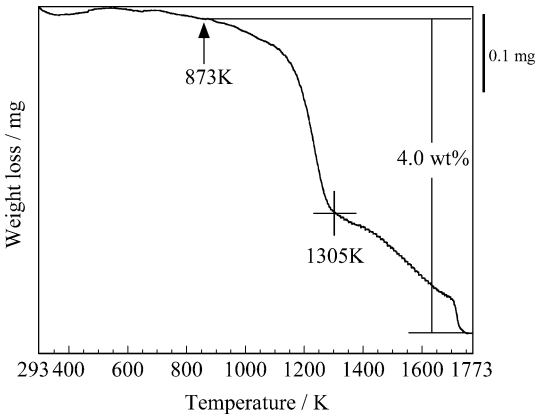

Fig. 1 Thermogravimetric curve for A-type carbonate apatite at 298–1773 K. Evolution of carbon dioxide began at 873 K and continued up to 1723 K; the amount was calculated to be 4.0 wt%

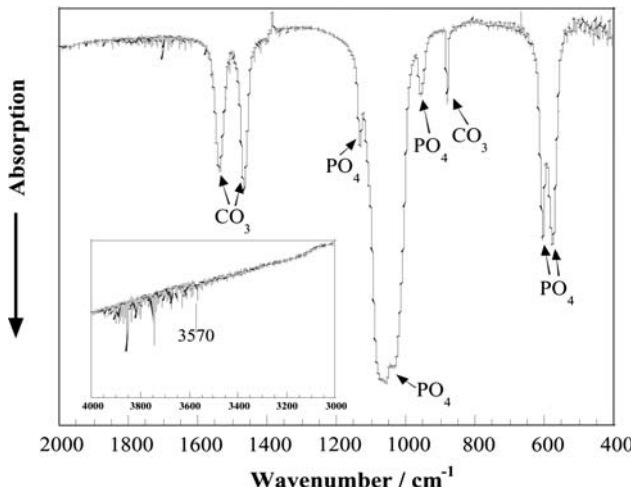

Fig. 2 Infrared absorption spectrum for A-type carbonate apatite completely substituted by carbonate ions. The typical absorption bands for A-type substitution are observed at 879, 1467 and 1539 cm^{-1}. The splitting of phosphate bands is clearly observed

1420–1540 cm^{-1} to the in-plane asymmetric stretch vibration mode (υ_3). The υ_2 and υ_3 bands of carbonate ions were observed at 879 cm^{-1} and at 1467 and 1539 cm^{-1}, respectively, while the OH bands at 3572 and 630 cm^{-1} were not detected. The absorption bands at 878 and 1460–1540 cm^{-1} were assigned to substitution at A-sites, while the bands at 871 and 1420–1470 cm^{-1} to substitution at B-sites [20–22]. Thus, the chemical formula of the powder sample prepared in this study was determined to be $Ca_{9.9\pm0.1}(PO_4)_{6.00\pm0.01}(CO_3)_{0.9\pm0.1}$.

Significant differences, namely, splitting of IR bands corresponding to PO_4^{3+}, υ_3, were observed between the A-type CAp and the stoichiometric HAp. In stoichiometric HAp, two υ_3 bands were observed at 1050 and 1092 cm^{-1} [17], whereas five υ_3 bands were clearly observed at 1029, 1039, 1055, 1075 and 1130 cm^{-1} in the present A-type CAp; the band at 1130 cm^{-1} was particularly intense. It was considered that the splitting of these υ_3 bands was due to the reduction of site symmetry accompanied by the lowering of space groups from monoclinic $P2_1/b$ to monoclinic Pb, as described below.

Crystal structure refinement and carbonate configuration

The apatite structures with space groups $P\bar{6}$ and $P\bar{3}$ were characterised by the [001] diffraction peak observed at 12.54° for the Cu Kα radiation [7–9]. In this study, the corresponding diffraction peak was observed at 12.865° and the extra diffraction peaks were simultaneously detected at 13.936°, 15.858°, 19.181°, 20.623°, 23.238°, 26.826°, 29.607°, 29.637°, 35.497° and 36.328°. Elliott et al. [10, 13] also observed all the extra diffraction peaks and proposed that A-type CAp had a monoclinic structure with space group Pb. The lattice parameters were determined to be $a = 0.9557$, $b \approx 2a$, $c = 0.6872$ nm and $\gamma = 120.36^\circ$ from powder XRD analyses. It is thus concluded from the detection of the extra diffraction peaks that the A-type CAp prepared in this study had the same analogy of space group Pb.

Possible models for the carbonate configuration are illustrated in Fig. 3. The carbonate configuration is the

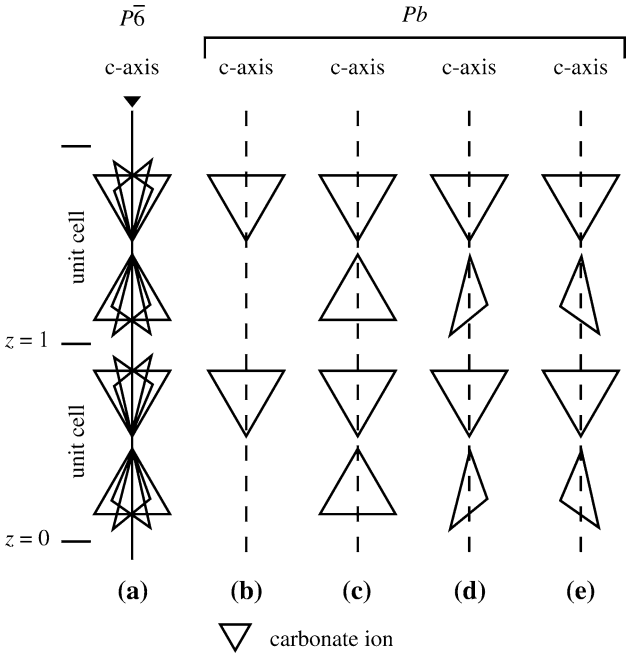

Fig. 3 Model arrangements for carbonate ions in A-type carbonate apatite: (*a*) disordered model for space group $P\bar{6}$, carbonate ions take three equivalent positions; (*b*) ordered model for space group Pb, carbonate ions arranged alternatively along the *c*-axis; (*c*–*e*) disordered model for space group Pb. In (*c*), each carbonate plane is arranged parallel to the *c*-axis

most important for determining the crystal structure. In model *a*, the carbonate ion stochastically occupies six equivalent positions because of the existence of both $\bar{6}$ axis and mirror planes ($z = 0, 1/2$) in space group $P\,\bar{6}$ [7–9]. On the contrary, there are *b*-glide planes instead of $\bar{6}$ and $\bar{3}$ axis in space group *Pb* (models *b*–*e*), and four configurations are possible for the carbonate ions. One (model *b*) is ordered and the other three models (*c*–*e*) are more or less stochastically disordered. In model *b*, the carbonate ions preferentially occupy one of two possible OH sites, maintaining an ordered arrangement such that all carbonate planes are parallel. In model *c*, the carbonate ions randomly occupy one of the two OH sites, though the planes are parallel to each other. In models *d* and *e*, the carbonate planes are alternately rotated about the *c*-axis.

Figure 4 shows the diffraction pattern (solid line) calculated for the ordered model together with that observed (dotted line). The inset arrows indicate the forbidden diffraction peaks for space groups $P\,\bar{6}$ and $P\,\bar{3}$. The agreement between the calculated and experimental data was insufficient, especially at the angles indicated by the open circles; in fact, the reliability factors (R_{wp} and R_p) and goodness of fit (*S* indicator) were only 11.07%, 7.77% and 1.81, respectively. The *S* indicator is defined as the R_{wp}/R_e value.

Table 1 gives the results of Rietveld refinement for model *c* (disordered). The values of R_{wp} and R_p values converged to 8.42 and 5.98%, respectively, and *S* indicator was less than 1.38. These values were sufficiently improved in comparison with those for the ordered model. The *a*-axis length calculated was 0.0014 nm longer than that reported [10], corresponding to the high concentration of carbonate ions in the present A-type CAp. Moreover, because twice the *a*-axis length is 0.0057 nm more than the *b*-axis length, all CO_3 planes are arranged in the same direction, i.e. parallel to the *a*-plane. Figure 5 shows the Rietveld refinement plots for model *c*. Comparing the miller indices, diffraction angles and relative intensities

Table 1 Rietveld refinement results for the A-type carbonate apatite

Compound	$Ca_{9.9\pm0.1}(PO_4)_{6.0\pm0.1}(CO_3)_{0.9\pm0.1}$
Space group	*Pb* (No. 7)
Z	2
Cell parameters (nm)	$a = 0.9571(1)$
	$b = 1.9085(2)$
	$c = 0.68755(3)$
	$\gamma = 119.847(7)$
Step scan increment/° 2θ	0.02
2θ range/° 2θ	10–110
No. of reflections (Cu $K\alpha_{1,\,2}$)	2954
No. of structure parameters	132
No. of profile parameters	24
R_{wp} (%)	8.42
R_p (%)	5.98
R_e (%)	6.08
R_I (%)	1.74
R_F (%)	0.95

estimated to those for model *b*, the agreement between the observed and calculated profiles is sufficiently good (see supplementary material). Therefore, it is considered that the arrangement of carbonate ions is disordered.

The refined atomic parameters are given in Table 2. There exist 10, 6 and 2 independent sites for Ca, PO_4 and carbonate ions, respectively. The thermal parameters refined were 1.16(4) for Ca, 1.19(6) for P and 0.90(9) for O. The Ca(1) to Ca(4) sites correspond to the Ca(1) site defined for space group $P6_3/m$, and similarly, the Ca(5) to Ca(10) sites to the Ca(2) site. For the carbonate ion, two independent sites are possible—*a*- and *b*-sites. The atomic positions of Ca^{2+} and PO_4^{3+} were fundamentally similar to those in monoclinic HAp [17].

The Rietveld refinements could not clearly distinguish between the three different models *c*–*e*. If the direction of carbonate planes had been disordered like in models *d* and

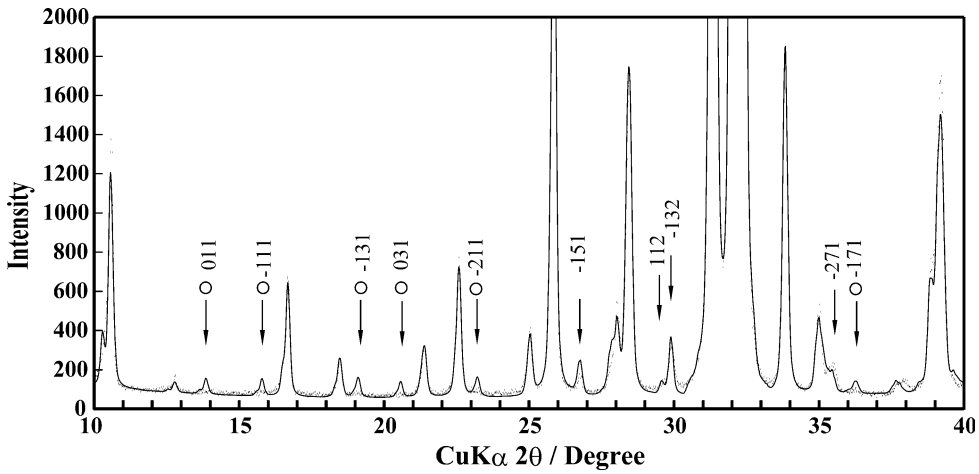

Fig. 4 Observed (*dots*) and calculated (*line*) patterns for A-type carbonate apatite with space group *Pb* where the carbonate ions are arranged in an orderly fashion (model *b*). The *circles* show characteristic and unfitted diffraction peaks

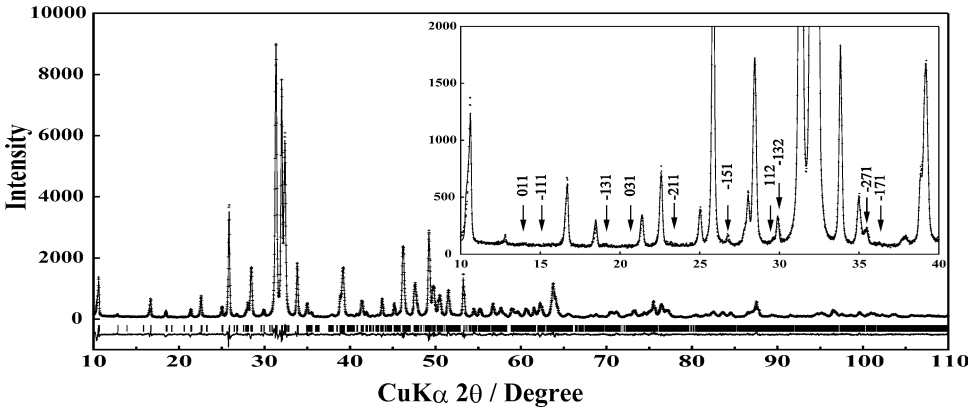

Fig. 5 Rietveld refinement plots for A-type carbonate apatite with space group *Pb* and disordered arrangement of carbonate ions. The carbonate arrangement used was model *c* in Fig. 4

e, twice the *a*-axis length should be nearly equal to the *b*-axis length due to the isotropic stereo-hindrance by the randomly located carbonate ions. However, since this was not the case, it is conjectured that the most possible configuration is the partially ordered model *c*.

The refined carbonate configuration for A-type CAp is illustrated in Fig. 6. The carbonate ions were disorderly arranged along the *c*-axis and *g* was determined to be 0.56(1) for the *a*-site and 0.34(1) for the *b*-site. All carbonate planes were almost parallel to the *c*- and *a*-axes, as shown in Fig. 6a**,** projected onto the (001) plane. In particular, one of the sides of the carbonate triangles was almost parallel to the *a*-axis, resulting in the elongation of the *a*-axis as mentioned above. Figure 6b illustrates the carbonate configuration (top view along *b*-axis). It was found that the adjacent carbonate triangles were oppositely rotated at the about the respective C atoms; the rotation angles were 23° at the *a*-site and −18° at the *b*-site. The feature of carbonate rotation in the apatite structure was almost coincident with the configuration calculated by computer modelling methods [23, 24]. It is worthy to note that, although the structural refinement using powder XRD data is inferior to single-crystal methods, the present carbonate configuration in which two oxygens are located on or close to the *c*-axis is in good agreement to the single-crystal study with trigonal space group $P\bar{3}$ described by Fleet and Liu [11, 12]. The reduction of space group $P\bar{6}$ to *Pb* was attributed to the rotational configuration of the carbonate ions: that is, the mirror planes at $z = 0$, 1/2 in space group $P\bar{6}$ did not appear in space group *Pb*.

Two independent Ca triangles constituted by Ca(5, 9 and 10) and by Ca(6, 7 and 8) existed at $z = 0$ and 1/2; the mean distances between the triangle planes calculated were 0.435 and 0.430 nm, respectively. This was caused by the above-mentioned two configurations of carbonate ions that were rotated by different angles: that is, the respective Ca ions in the triangles shifted by different distances via attractive forces from the adjacent O ions in the carbonate ions. For example, the distance was 0.204(2) nm (Ca(10)–O(a2)) and 0.206(2) nm (Ca(5)–O(a3)) and 0.197(2) nm (Ca(8)–O(b2)).

The slant of a carbonate ion in A-type CAp against the *c*-axis has been reported to be 27° using polarised IR spectroscopy [13]. In this study, the slant was vague because of the distortion of the carbonate plane, i.e. the vertical displacement of C atom from the triangular plane together with O atoms. This could cause the disappearance of mirror planes in space group $P\bar{6}$.

Relationship between chemical composition and space group

From the results of HAp structural analyses, the relationships between Ca or OH deficiency and space groups are summarised as follows. Stoichiometric HAp with a Ca/P ratio between 1.65 and 1.67 has monoclinic symmetry with space group $P2_1/b$ ($a = 0.9426$, $b = 1.8856$, $c = 0.6887$ nm and $\gamma = 119.97°$) [17, 25], whereas HAp with Ca deficiency (Ca/P ratio < 1.65) has hexagonal symmetry with space group $P6_3/m$ ($a = 0.9421$, $c = 0.6881$ nm) [26]. Although both space groups are centrosymmetric, their structures are distinguished by the arrangement of ions in the OH channel: OH–OH–OH–OH… (ordered) or OH–HO–OH–HO…(disordered). Such arrangement strongly depended on the amount of Ca deficiency. In the $P2_1/b$ system, the origin of the unit cell was shifted by (0, −1/2, 0) from that of $P6_3/m$, and the *b*-axis was about twice as long as the *a*-axis because of the appearance of a *b*-glide plane. Further the 6_3 axis disappeared and the mirror plane changed in the 2_1 axis. Furthermore, oxyhydroxyapatites obtained by >33% dehydration of HAp had triclinic symmetry with space group $P\bar{1}$ with lattice parameters $a = 0.94002$, $b = 0.93970$, $c = 0.68996$, $\alpha = 90.063$, $\beta = 89.747$ and $\gamma = 119.99$ [19]. The disturbance in the arrangement of ions in the OH channel and the degree of Ca deficiency are critical to determining the crystal structure of HAp.

When the OH sites in HAp were partially occupied by carbonate ions and HAp contained a small amount of O or

Table 2 Structural parameters for the A-type carbonate apatite

Atom	*x*	*y*	*z*
Ca^{2+}(1)	0.340(12)	0.593(4)	0.251(2)
Ca^{2+}(2)	0.338(12)	0.580(4)	0.736(1)
Ca^{2+}(3)	0.656(12)	0.410(4)	0.736(1)
Ca^{2+}(4)	0.676(12)	0.423(4)	0.253(2)
Ca^{2+}(5)	0.260(13)	0.245(4)	−0.003(2)
Ca^{2+}(6)	−0.005(12)	0.618(4)	0.498(2)
Ca^{2+}(7)	0.262(13)	0.376(4)	0.499(2)
Ca^{2+}(8)	0.735(13)	0.255(4)	0.493(3)
Ca^{2+}(9)	0.014(12)	0.368(4)	−0.012(2)
Ca^{2+}(10)	0.732(13)	0.123(4)	−0.002(2)
P(1)	0.392(12)	0.435(4)	0.002(2)
P(2)	0.634(12)	0.272(4)	0.003(2)
P(3)	0.032(12)	0.457(4)	0.496(2)
P(4)	0.590(13)	0.061(4)	0.495(2)
P(5)	0.376(13)	0.236(4)	0.495(2)
P(6)	0.970(13)	0.057(3)	0.009(2)
O^{-}(1)	0.325(12)	0.495(4)	0.014(5)
O^{-}(2)	0.573(13)	0.479(4)	−0.063(4)
O^{-}(3)	0.383(14)	0.398(5)	0.204(3)
O^{-}(4)	0.293(13)	0.365(4)	0.854(4)
O^{-}(5)	0.534(12)	0.179(5)	−0.022(4)
O^{-}(6)	0.515(15)	0.304(5)	0.047(5)
O^{-}(7)	0.728(13)	0.315(4)	0.811(3)
O^{-}(8)	0.763(13)	0.297(4)	0.171(3)
O^{-}(9)	0.854(11)	0.433(4)	0.492(4)
O^{-}(10)	0.140(12)	0.548(4)	0.467(4)
O^{-}(11)	0.079(14)	0.435(4)	0.690(4)
O^{-}(12)	0.074(14)	0.414(4)	0.333(6)
O^{-}(13)	0.654(13)	−0.001(3)	0.502(4)
O^{-}(14)	0.407(12)	0.018(4)	0.514(5)
O^{-}(15)	0.668(13)	0.124(4)	0.664(5)
O^{-}(16)	0.634(13)	0.108(4)	0.304(3)
O^{-}(17)	0.488(13)	0.327(4)	0.512(4)
O^{-}(18)	0.471(14)	0.189(4)	0.511(5)
O^{-}(19)	0.286(13)	0.213(2)	0.301(2)
O^{-}(20)	0.246(12)	0.210(4)	0.661(3)
O^{-}(21)	0.157(8)	0.593(4)	−0.011(3)
O^{-}(22)	0.892(13)	0.968(6)	−0.042(5)
O^{-}(23)	0.907(13)	0.066(4)	0.211(5)
O^{-}(24)	0.924(13)	0.104(4)	0.857(3)
C(a)	−0.013(13)	0.254(4)	0.249(5)
O^{-}(a1)	0.021(15)	0.248(6)	0.426(6)
O^{-}(a2)	−0.160(13)	0.214(5)	0.197(7)
O^{-}(a3)	0.095(15)	0.271(5)	0.121(7)
C(b)	−0.044(16)	0.235(6)	0.712(8)
O^{-}(b1)	0.015(14)	0.244(8)	0.541(10)
O^{-}(b2)	−0.168(16)	0.243(7)	0.735(10)
O^{-}(b3)	0.049(15)	0.250(8)	0.858(12)

OH ions, the resultant A-type CAp had hexagonal symmetry with space group $P\bar{6}$ ($a = 0.9530$, $c = 0.6887$ nm) [7–9]. A-type CAp with space group $P\bar{6}$ has 4, 2 and 1 independent sites for Ca, PO_4 and carbonate ions. Furthermore, A-type CAp with space group $P\bar{3}$ ($a = 0.95211$, $c = 0.6725$ nm) [11, 12] has 3 and 1 independent sites for Ca^{2+} and carbonate ions, including 1 P site and 4 O sites in the PO_4 ions. On the contrary, the A-type CAp completely substituted by the carbonate ion had monoclinic symmetry with space group *Pb* [10]; the present sample belongs to this category. The origins of the unit cells of $P\bar{6}$ and *Pb* were shifted at $z = 1/4$ along the *c*-axis from those of $P6_3/m$ and $P2_1/b$ for the HAp, respectively. However, the origin of $P\bar{3}$ for the A-type CAp was same to those of $P6_3/m$ and $P2_1/b$ for the HAp. The relationship between space groups $P\bar{6}$ and *Pb* was quite similar to that between $P2_1/b$ and $P6_3/m$: that is, the $\bar{6}$ axis of $P\bar{6}$ disappeared in *Pb*, and simultaneously the mirror planes at $z = 0$ and 1/2 were converted to the *b*-glide planes.

With respect to single crystals and powders of A-type CAp, different structures were proposed. Young et al. [27] and Suetsugu et al. [9, 28] studied on the A-type CAp completely substituted by carbonate ions using neutron and/or X-ray diffraction techniques. The crystal structures were analysed on the basis of the hexagonal space groups, $P6_3/m$ and $P\bar{6}$, respectively, being different from the result of *Pb* for the powder CAp. The single crystal of A-type CAp, belonged to space group $P\bar{6}$ [9], had carbonate ions at both PO_4 and OH sites together with a small Ca^{2+} deficiency at 0.25/10. Furthermore, Fleet and Liu [11, 12] determined the crystal structure of the A-type CAp single crystal including 0.25 mol of the OH ions at the channels. The single crystal exhibited the trigonal space group group $P\bar{3}$. These results suggest that the crystal structure of apatite is delicately varied with its chemical composition, and particularly with the degree of deficiency in the constituents Ca and OH, the type of sites occupied by carbonate ions and the presence of impurities such as O ions.

Phase transition

A-type CAp with complete substitution by carbonate ions showed reversible phase transition from a monoclinic to hexagonal lattice near 473 K [13, 14]. This phase transition was ascribed to the disappearance of the *b*-glide plane accompanying the change in carbonate arrangement, i.e. the transition from an ordered state to a threefold rotational disordered state along the *c*-axis. However, in this study, no endo/exothermic peaks were observed for the A-type CAp as shown in Fig. 7 (DSC curve), indicating that the crystal structure could not change via the displacement of

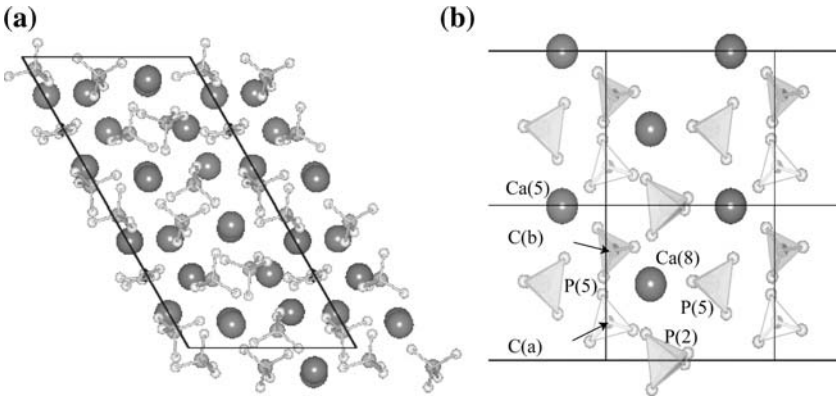

Fig. 6 Projection of the refined atomic configuration for A-type carbonate apatite onto **a** the (001) plane and **b** the (010) plane. The *solid line* shows the unit cell of A-type carbonate apatite

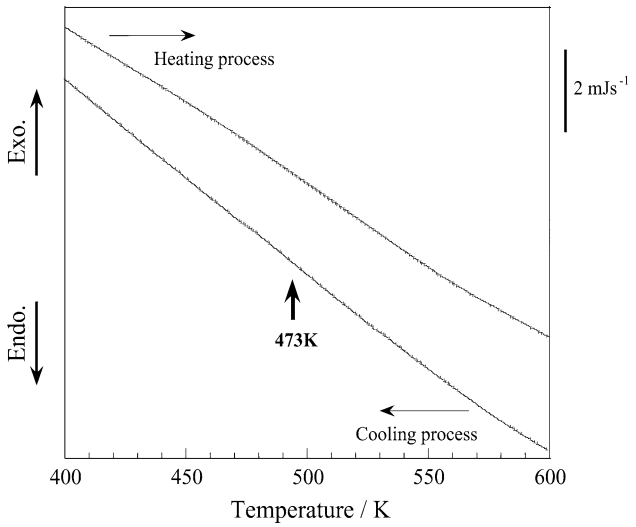

Fig. 7 Differential scanning calorimetric curves for A-type carbonate apatite at heating and cooling rates of 20 K/min

carbonate ions. It could be attributed to stereochemical hindrance at low temperature in model *c* (Fig. 3).

Conclusions

The crystal structure of A-type CAp ($Ca_{9.9\pm0.1}(PO_4)_{6.00\pm0.1}(CO_3)_{0.9\pm0.1}$) was determined by Rietveld refinements using powder X-ray diffraction data. The crystal structure was monoclinic with space group *Pb*; the lattice parameters were $a = 0.9571(1)$, $b = 1.9085(2)$, $c = 0.68755(3)$ nm and $\gamma = 119.847(7)°$. There existed two different carbonate sites that were oppositely rotated about the corresponding carbon atoms by 23° and −18°. The configuration of carbonate ions was thus not ordered, but disordered along the *c*-axis; however, all carbonate planes were almost parallel to the *a*-axis. The amount of Ca deficiency, the type of sites occupied by carbonate ions, and degree of substitution by carbonate at OH sites had a strong influence on the crystal structure and carbonate configuration in A-type CAp. No thermal phase transition was detected.

References

1. LeGeros RZ, Trautz OR, LeGeros JP, Klein E (1969) Cell Mol Life Sci 15:5
2. LeGeros RZ (1994) In: Brown PW, Constantz B (eds) Hydroxyapatite and related materials. CRC Press Inc., Boca Raton
3. Lee JC, Cho SB, Lee SJ, Rhee SH (2009) J Mater Sci 44:4531. doi:10.1007/s10853-009-3685-3s
4. Barralet JE, Fleming GJP, Campion C, Harris JJ, Wright AJ (2003) J Mater Sci 38:3979. doi:10.1023/A:1026258515285
5. Barinov SM, Rau JV, Cesaro SN, Durisin J, Fadeeva IV, Ferro D, Medvecky L, Trionfetti G (2006) J Mater Sci Mater Med 17:597
6. Komlev VS, Fadeeva IV, Gurin AN, Kovaleva ES, Smirnov VV, Gurin NA, Barinov SM (2009) Inorg Mater 45:329
7. Ikoma T, Kubo Y, Yamazaki A, Akao M, Tanaka J (2001) Key Eng Mater 192-5:191
8. Ito A (1988) Crystal growth and structure of apatitic phosphates. PhD Thesis, Waseda University
9. Suetsugu Y, Takahashi Y, Okamura FP, Tanaka J (2000) J Solid State Chem 155:292
10. Elliott JC (1980) J Appl Crystallogr 13:618
11. Fleet ME, Liu X (2003) J Solid State Chem 174:412
12. Fleet ME, Liu X (2005) Biomaterials 26:7548
13. Elliott JC (1994) Structure and chemistry of the apatites and other calcium orthophosphates. Elsevier Press, Amsterdam
14. Trombe JC (1973) Ann Chim (Paris) 14th Series 8:251
15. Bonel G (1972) Ann Chim (Paris) 14th Series 7:65
16. Bonel G (1972) Ann Chim (Paris) 14th Series 7:127
17. Ikoma T, Yamazaki A, Nakamura S, Akao M (1999) J Solid State Chem 144:272
18. Izumi F, Ikeda T (2000) Mater Sci Forum 321–324:198
19. Alberius-Henning P, Adolfsson E, Grins J, Fitch A (2001) J Mater Sci 36:663. doi:10.1023/A:1004876622105s
20. Rey C, Collins B, Goehl T, Dickson IR, Glimcher MJ (1989) Calcif Tissue Int 45:157
21. Rey C, Renugopalakrishnan V, Collins B, Glimcher MJ (1991) Calcif Tissue Int 49:251
22. Rey C, Shimizu M, Collins B, Glimcher MJ (1991) Calcif Tissue Int 49:259

23. Peroos S, Du Z, Henriette de Leeuw N (2006) Biomaterials 27:2150
24. Astala R, Stott MJ (2005) Chem Mater 17:4125
25. Elliott JC (1973) Science 180:1055
26. Kay MI, Young RA, Posner AS (1964) Nature 204:1050
27. Young RA, Bartlett ML, Spooner S, Mackie PE (1981) J Biol Phys 9:1
28. Suetsugu Y, Shimoya I, Tanaka J (1998) J Am Ceram Soc 81:746